© 2021. Published by The Company of Biologists Ltd | Development (2021) 148, dev189753. doi:10.1242/dev.189753

STEM CELLS AND REGENERATION

RESEARCH ARTICLE

ERECTA family signaling constrains *CLAVATA3* and *WUSCHEL* to the center of the shoot apical meristem

Liang Zhang*,[1], Daniel DeGennaro[1], Guangzhong Lin‡,[2], Jijie Chai[2,3,4] and Elena D. Shpak[1,§]

ABSTRACT

The shoot apical meristem (SAM) is a reservoir of stem cells that gives rise to all post-embryonic above-ground plant organs. The size of the SAM remains stable over time owing to a precise balance of stem cell replenishment versus cell incorporation into organ primordia. The WUSCHEL (WUS)/CLAVATA (CLV) negative feedback loop is central to SAM size regulation. Its correct function depends on accurate spatial expression of *WUS* and *CLV3*. A signaling pathway, consisting of ERECTA family (ERf) receptors and EPIDERMAL PATTERNING FACTOR LIKE (EPFL) ligands, restricts SAM width and promotes leaf initiation. Although ERf receptors are expressed throughout the SAM, EPFL ligands are expressed in its periphery. Our genetic analysis of *Arabidopsis* demonstrated that ERfs and CLV3 synergistically regulate the size of the SAM, and *wus* is epistatic to ERf genes. Furthermore, activation of ERf signaling with exogenous EPFLs resulted in a rapid decrease of *CLV3* and *WUS* expression. ERf-EPFL signaling inhibits expression of *WUS* and *CLV3* in the periphery of the SAM, confining them to the center. These findings establish the molecular mechanism for stem cell positioning along the radial axis.

KEY WORDS: *Arabidopsis*, Stem cells, Signaling, ERECTA, Plant development, Shoot apical meristem

INTRODUCTION

The shoot apical meristem (SAM) generates new organs throughout the life of a plant. As stem cells in the central zone of the dome-shaped SAM slowly divide, some of their progeny are displaced laterally into the peripheral zone and basally into the rib zone. Cells in the peripheral and rib zones rapidly divide, differentiate and are incorporated into forming leaves, flowers and stems. Even though cells are constantly dividing, the SAM size remains stable throughout development owing to a tight balance of proliferation and incorporation of cells into new organs.

The principal regulator of SAM size is a negative feedback loop consisting of WUSCHEL (WUS; AT2G17950) and CLAVATA3 (CLV3; AT2G27250) (Fuchs and Lohmann, 2020). WUS is a homeodomain transcription factor that maintains the pool of stem cells; in its absence stems cells arise but almost immediately differentiate (Laux et al., 1996). *WUS* is expressed in the organizing center beneath the central zone, and the protein moves up into the central zone through plasmodesmata (Brand et al., 2000; Daum et al., 2014; Mayer et al., 1998; Schoof et al., 2000; Yadav et al., 2011). *CLV3* encodes a secreted peptide expressed in the central zone and perceived by multiple plasma membrane localized receptors: CLV1 (AT1G75820), CLV2, BARELY ANY MERISTEM 1 (BAM1; AT5G65700), BAM2 (AT3G49670), CORYNE (CRN), RECEPTOR-LIKE PROTEIN KINASE 2 (RPK2) and CLAVATA3 INSENSITIVE RECEPTOR KINASEs (CIKs) (DeYoung et al., 2006; Fletcher et al., 1999; Hu et al., 2018; Kinoshita et al., 2010; Müller et al., 2008; Shinohara and Matsubayashi, 2015). In the central zone, WUS binds directly to the promoter of *CLV3* and activates its expression while CLV3-activated signaling inhibits *WUS* expression (Brand et al., 2000; Schoof et al., 2000; Yadav et al., 2011), forming a regulated feedback loop.

One of the central questions to understanding the meristem is how the spatial expressions of *CLV3* and *WUS* are established and maintained in the face of the continual turnover of cells. Previous studies have elucidated key mechanisms underlying the apical-basal distributions of *CLV3* and *WUS*. The depth of the *WUS* expression domain is defined by opposing activity of CLV3 and cytokinin: CLV3 inhibits *WUS* expression whereas cytokinin signaling promotes it. Both signals are produced in the apical region of the meristem and form a diffusion gradient along the apical basal axis. Cytokinin is perceived in deeper tissue layers than CLV3, which establishes *WUS* expression at a certain distance from the surface of the SAM (Chickarmane et al., 2012). Confinement of *CLV3* expression to the region above the *WUS* domain is dependent on HAIRY MERISTEM (HAM) transcription factors in the rib zone. Interaction with HAM transcription factors prevents WUS from activating *CLV3* transcription, which restricts *CLV3* expression to the apical region of the SAM (Zhou et al., 2018). However, it remains unclear why *WUS* and *CLV3* are expressed only around the central vertical axis of the SAM. Previous mathematical models have used implicit or explicit assumptions to define the lateral boundary that confines the expression of *WUS* and *CLV3* (Gruel et al., 2018; Zhou et al., 2018), but little is known about the actual existence of such a lateral signal. A recent model of SAM growth in the *clv3* mutant suggested the existence of additional mechanisms sustaining the peripheral zone (Klawe et al., 2020). Here, we present data showing that ERECTA family signaling restricts *WUS* and *CLV3* expression laterally, confining them to the center of the meristem thereby providing a key mechanism for SAM maintenance.

ERECTA (*ER*; AT2G26330), *ERECTA-LIKE 1* (*ERL1*; AT5G62230) and *ERL2* (AT5G07180), collectively called ERfs, encode plasma membrane-localized leucine-rich repeat receptor-like kinases (Shpak et al., 2004). The activity of ERf receptors is regulated by a group of cysteine-rich peptides belonging to the

[1]Department of Biochemistry, Cellular and Molecular Biology, University of Tennessee, Knoxville, TN 37996, USA. [2]Beijing Advanced Innovation Center for Structural Biology, Tsinghua-Peking Joint Center for Life Sciences, Center for Plant Biology, School of Life Sciences, Tsinghua University, 100084 Beijing, China. [3]Max Planck Institute for Plant Breeding Research, 50829 Cologne, Germany. [4]Institute of Biochemistry, University of Cologne, Zuelpicher Strasse 47, 50674 Cologne, Germany.
*Present address: Complex Carbohydrate Research Center, University of Georgia, Athens, GA 30602, USA. ‡Present address: No. 4 Building No. 50, Huatuo Road, Daxing District, Beijing 102629, China.

§Author for correspondence (eshpak@utk.edu)

E.D.S., 0000-0002-5702-7517

Handling Editor: Ykä Helariutta
Received 25 February 2020; Accepted 8 February 2021

Development (2021) 148, dev189753. doi:10.1242/dev.189753

EPIDERMAL PATTERNING FACTOR/EPF-LIKE (EPF/EPFL) family (Hara et al., 2007, 2009; Lee et al., 2012; Lin et al., 2017). A mitogen-activated protein kinase cascade consisting of YODA, MKK4/5/7/9 and MPK3/6 functions downstream of the receptors (Bergmann et al., 2004; Lampard et al., 2009, 2014; Meng et al., 2012; Wang et al., 2007). ERf signaling controls various developmental processes including stomata formation, above-ground organ elongation, SAM size, leaf initiation and phyllotaxy (Chen et al., 2013; Shpak, 2013; Uchida et al., 2013). In the SAM, three ERfs function redundantly, with single and double mutants having no or extremely weak meristematic phenotypes. Altered meristem development can be observed in the *er erl1 erl2* mutant, which has a wider vegetative SAM and forms fewer leaves at almost random divergence angles (Chen et al., 2013; Uchida et al., 2013). Recently, we demonstrated that ERf activity in the SAM is controlled by four ligands – EPFL1 (AT5G10310), EPFL2 (AT4G37810), EPFL4 (AT4G14723) and EPFL6 (AT2G30370) – which are expressed at the periphery of the SAM (Kosentka et al., 2019). In-depth transcriptome profiling of *Aquilegia coerulea* identified a homolog of *EPFL4* as a most connected hub in the flower meristem gene network, further confirming the importance of EPFL4 for meristem maintenance (Min and Kramer, 2020).

Based on altered expression of DR5rev:GFP and PIN1pro:PIN1-GFP markers in *er erl1 erl2*, we proposed that the decrease in leaf initiation might be a result of altered auxin distribution (Chen et al., 2013); the cause of the increased meristem size, however, has remained unknown. A decrease in organ initiation does not automatically lead to an increase of SAM size. For example, the inflorescence meristem of the *pin1* mutant does not show alteration of size or *WUS* expression, although it fails to produce flower organs (Vernoux et al., 2000). As regulation of SAM size depends on the CLV3/WUS feedback loop, we investigated whether ERfs genetically interact with these two genes and alter their expression. Our experiments indicate that ERfs are important modulators of *CLV3* and *WUS* expression. We propose that ERf and EPFLs are a part of a new regulatory circuit that enables communication between the peripheral and the central zones and specifies the location and size of the stem cell population in the SAM.

RESULTS

ERf/EPFL and CLV3 signaling synergistically restrict SAM size

In a previous study, 10-day old *clv3 er erl1 erl2* seedlings had a bigger SAM compared with both *er erl1 erl2* and *clv3* (Kimura et al., 2018). Here, we investigate how the ERf and CLV3 signaling pathways control meristem maintenance over time and their effect on leaf initiation and internode formation. Comparison of *clv3* with *er erl1 erl2* mutants suggests that, although both ERfs and CLV3 control SAM size, they play dominant roles during different developmental stages. At 1 day post germination (DPG) the SAM of *er erl1 erl2* is considerably wider (105.1±3.3; mean±s.e.m.) than in the wild type (56.1±1.7; $P<1.2\times10^{-13}$ in unpaired two-tailed Student's *t*-test) or in *clv3* (83.0±1.4; $P<4.2\times10^{-7}$) (Fig. 1A,C), suggesting a key role for ERfs in restricting SAM size during embryogenesis. For the first 5 days after germination, the wild type and *er erl1 erl2* SAMs do not substantially further increase in width whereas *clv3* SAM size continues to increase, indicating that post embryogenesis CLV3 signaling plays the primary role in SAM size maintenance (Fig. 1A). The two pathways also contribute differently to leaf initiation, with ERfs promoting leaf initiation and CLV3 slightly inhibiting it (Fig. 1B).

The most dramatic phenotype is observed when both signaling pathways are deactivated. The *clv3 er erl1 erl2* mutant has a considerably larger SAM immediately after germination (Fig. 1A). Post embryonically, the SAM increases dramatically in size but does not form lateral organs and internodes (Fig. 1D,E). In rare occasions the mutant will form one or two leaves or produce structures resembling stigmas, but it never forms a stem even after more than 40 days of growth (Fig. S1A,B). The meristematic nature of the dome-like structure in *clv3 er erl1 erl2* is consistent with the presence of cells with dense cytoplasm and without chlorophyll in the outer cell layers (Fig. 2A; Fig. S1C). Moreover, the epidermal layer is composed of very small cells and the guard cells are absent, indicating absence of differentiation (Fig. S1D). The synergistic function of CLV3 and ERfs in the SAM is also evident in the *clv3 er erl2* mutant: although the *er erl2* mutant has a meristem indistinguishable from the wild type, these two mutations enhance the width of the *clv3* SAM, and *er erl2* reduces leaf initiation in the *clv3* background (Fig. S1E,F). Finally, CLV3 regulates SAM size and leaf initiation in concert with the meristematic ERf ligands EPFL1, EPFL2, EPFL4 and EPFL6. The size of the SAM is dramatically increased in *clv3 epfl1 epfl2 epfl4 epfl6* plants, comparable with the increase we observed in *clv3 er erl1 erl2* mutants (Fig. 1F). Similar to our previous findings (Kosentka et al., 2019), the four EPFLs function redundantly in regulation of SAM size, as we observed a drastic increase only in the pentuple *clv3 epfl1 epfl2 epfl4 epfl6* mutant.

Taken together, these findings indicate that ERf and CLV3 signaling pathways synergistically restrict SAM size. The extent of their individual contributions varies at different developmental stages. Before germination both contribute to SAM width maintenance with ERfs playing the primary role. After germination their roles switch, with CLV3 playing the dominant role and ERf signaling becoming auxiliary. In addition, synergistic function of ERf and CLV3 is essential for differentiation of organs at the periphery of the meristem and for growth of internodes.

The *wus* mutation is epistatic to *er erl1 erl2*

CLV3 regulates meristem size by inhibiting expression of *WUS* (Brand et al., 2000; Müller et al., 2006; Schoof et al., 2000). Although expression of *WUS* is increased in an *er erl1 erl2* background, the increase is relatively moderate: four- to six-fold at 5 DPG (Chen et al., 2013; Uchida et al., 2013) (Fig. 1G). The significance of ERfs for regulation of *WUS* expression becomes more evident in the absence of CLV3 signaling. In 5 DPG *clv3 er erl1 erl2* seedlings we observed up to ∼30-fold increase in *WUS* expression compared with the single *clv3* mutation and a ∼1000-fold increase over the wild type (Fig. 1G). The massive increase of *WUS* expression in *clv3 er erl1 erl2* is unlikely to be due simply to a bigger meristem size, as the other meristematic marker *STM* increases only ∼5.5-fold compared with *clv3* and 11-fold compared with the wild type. The large increase of *WUS* expression in *clv3 er erl1 erl2* suggests that its expression is synergistically regulated by CLV3 and ERfs.

To study genetic interactions between *ERfs* and *WUS* and to compare them with *CLV3* and *WUS* genetic interactions, we measured SAM size in *wus*, *wus er erl1 erl2*, *wus clv3* and *wus clv3 er erl1 erl2* mutants at 3 and 5 DPG. Although SAM width varied in individual seedlings (Fig. S2A), the four mutants were statistically indistinguishable (Fig. 2B) suggesting that during early seedling growth *wus* is epistatic to both *clv3* and *er erl1 erl2*. This conclusion is supported by histological analysis: the shoot apices of *wus*, *wus er erl1 erl2* and *wus clv3 er erl1 erl2* mutants did not have the classic dome-like SAM structure consisting of multiple layers of small, evenly shaped and tightly packed stem cells (Fig. 2A). In the mutants, the shoot apices were composed of only two layers of small cells with some of those cells dividing periclinally, a sign of

Development (2021) 148, dev189753. doi:10.1242/dev.189753

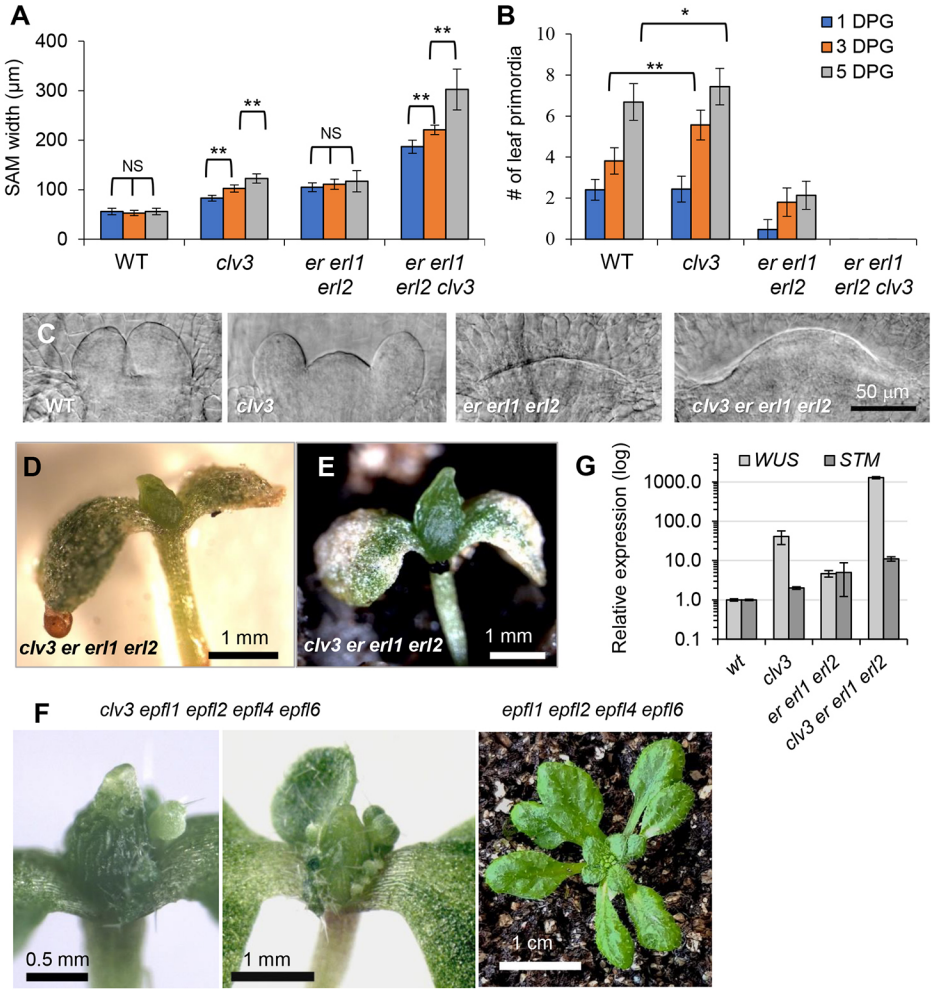

Fig. 1. *CLV3* and ERfs synergistically regulate SAM size and leaf initiation. (A,B) Comparison of SAM width (A) and leaf initiation (B) at 1,3 and 5 days post germination (DPG) in wild-type (WT) and mutants. The rate of leaf primordia initiation was determined by DIC microscopy of fixed samples. A primordium was defined as a bulge over 15 µm. Data are mean± s.e.m.; *n*=6-18. **P*<0.05, ***P*<0.001, NS, no statistically significant difference (unpaired two-tailed Student's *t*-test). An absence of bars for *er erl1 erl2 clv3* in B represent a complete absence of leaf primordia in that genotype at that age. (C) The SAM of dark grown seedlings at 1 DPG. All images are at the same magnification. (D) 29 DPG plant. (E) 42 DPG plant. (F) 19 DPG seedlings. (G) RT-qPCR analysis of *WUS* and *STM* in above-ground organs of 5 DPG seedlings of wild-type (WT) and mutants as indicated. Data are mean±s.d. *ACTIN2* was used as an internal control.

premature differentiation (Fig. S2B). A previous analysis of *wus er erl1 erl2* using 10 DPG seedlings indicated that its SAM is bigger than that of *wus*, suggesting additive effects of *ERf* and *WUS* (Kimura et al., 2018). This conclusion was supported by the ability of *er erl1 erl2* mutations to partially rescue initiation of stamens and carpels in the *wus* background (Kimura et al., 2018). However, our data and analysis of *wus er erl1 erl2* does not support the hypothesis of additive *ERf* and *WUS* interactions. At 10 DPG in many *wus er erl1 erl2* seedlings we observed a narrow region between forming leaf primordia (Fig. S2C). Although in some seedlings the area between forming leaves was indeed large, it did not contain stem cells with the characteristic dense cytoplasm (Fig. S2C). Based on morphology, cells in that region are differentiated: they are highly vacuolated, and some L2 layer cells divide in orientations other than anticlinal. We did occasionally observe meristem-like aggregations of small cells with dense cytoplasm; however, those structures were always small in diameter and asymmetrically localized, often at the axil of a leaf. These structures may be either axillary meristems or leaf primordia arising from a few erratically localized stem cells. Thus, although initiation of new meristematic regions or leaf primordia might be altered in *wus er erl1 erl2* compared with *wus*, there is no rescue of the central zone maintenance. Our analysis of *wus er erl1 erl2* flower structure in 2-month-old plants indicated that ERf family mutations were unable to rescue carpel or stamen initiation in the *wus* background (Table S1). While analyzing flower development we observed formation of stigma-like structures at the tips of sepals and the formation of stigma-like tissue in the area of the shoot apex in older *wus er erl1 erl2* plants, but in flowers that emerge soon after bolting we never observed the formation of carpels. Although we used the same alleles of *WUS* and ERfs, we cannot reproduce the *wus er erl1 erl2* flower structure data described by Kimura and colleagues (Kimura et al., 2018). In sum, our data indicate that *wus* is epistatic to *er erl1 erl2* in regulation of the SAM central zone width and in the flower meristem.

ERf restricts lateral expression of *CLV3* and *WUS*

In situ RNA hybridization and GUS reporter analysis show an increased expression of *CLV3* and *WUS* in the vegetative SAM of *er erl1 erl2* mutants (Kimura et al., 2018; Uchida et al., 2013). To quantify the spatial expression of these two genes we generated transgenic plants expressing nuclear localized EGFP (H2B-EGFP) under the *CLV3* and *WUS* cis-regulatory sequences. Fluorescent reporter analysis suggests that the *CLV3* expression domains in the wild type and in *er erl2* mutants are very similar (Fig. 3A), consistent with the indistinguishable SAM size in the wild type and the mutant during seedling development (Chen et al., 2013). In the 1-day old seedlings, the *CLV3* reporter was expressed in the L1 epidermal layer, the L2 subepidermal layer and in top two cell layers of the L3 zone. When seen from overhead, the *CLV3* reporter expression region appears oval; it is slightly broader along the axis connecting the boundaries of cotyledons (width #1 in Fig. 3B,C). In the *er erl1 erl2* mutant, the expression of the *CLV3* reporter is expanded more than twice in both directions, along the shorter and longer axes, leading to a dramatic increase in the lateral area of expression. In addition, we

Development (2021) 148, dev189753. doi:10.1242/dev.189753

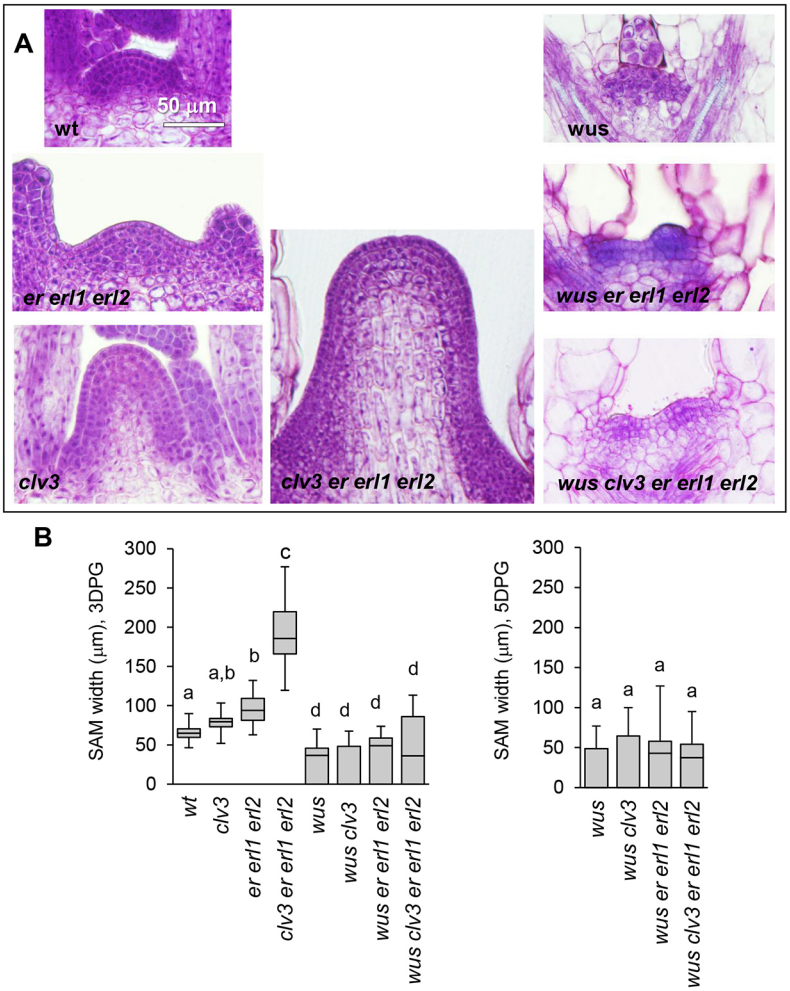

Fig. 2. *wus* is epistatic to *er erl1 erl2*. (A) Median sections of shoot apices of 5 DPG wild-type (wt) and mutant seedlings. All images are at the same magnification. (B) SAM width measurements performed by DIC microscopy using 3 DPG (left) and 5 DPG (right) seedlings. n=15-36. The median is indicated as a thick horizontal line, upper and lower quartiles are represented by the boxes, and the vertical lines designate the maximum and the minimum. For multiple comparisons (one-way ANOVA with Tukey post-hoc test), lower case letters are used to label means, such that bars bearing different letters are statistically different from one another with a minimum P-value of <0.01.

often observed extended expression of the *CLV3* reporter in the L1 layer in the periphery of the SAM (Fig. 3A) as has been reported previously (Kimura et al., 2018). The *er erl1erl2* mutations had only minor (if any) impact on the depth of *CLV3* expression.

Next, we analyzed the expression of the *WUS* reporter. In the *er erl2* mutant the reporter was expressed in the top two cell layers of the L3 zone (Fig. 4A). When seen from above, the area of expression was oval, similar to the *CLV3* expression, but smaller in size. The expression of our *WUS* reporter just below the L2 layer in the SAM is consistent with previously published data for the wild type (Daum et al., 2014; Mayer et al., 1998). As the expression of the *WUS* reporter was inconsistent and difficult to detect in the wild-type seedlings, we crossed transgenic *er erl2* with the wild type and analyzed expression of the reporter in the F1 generation. As both *er* and *erl2* are recessive mutations and F1 has a wild-type phenotype we called these seedlings WT on Fig. 4. The pattern of *WUS* expression in the wild type and *er erl2* was indistinguishable (Fig. 4B). However, in the *er erl1 erl2* mutant there was a dramatic increase in the reporter expression in the lateral direction (Fig. 4). We did not observe significant changes in the reporter expression along the apical-basal axis. Taken together, our analysis of *WUS* and *CLV3* expression in the *er erl1 erl2* mutant suggests that ERf signaling laterally restricts the expression of these two genes.

ERf signaling directly inhibits expression of *CLV3* and *WUS*

The very broad expression of *CLV3* in the L1 layer of the *er erl1 erl2* mutant is difficult to explain simply by expansion of the central zone. Although *epfl1 epfl2 epfl4* and *epfl1 epfl2 epfl6* mutants exhibit only a ∼1.25-fold increase in SAM width compared with the wild type (Kosentka et al., 2019), they express four to six times more *CLV3* (Fig. 5A). These facts coupled with the epistatic nature of the *wus* mutation motivated us to investigate whether *WUS* and *CLV3* are the direct targets of the ERf signaling pathway. We treated *epfl1 epfl2 eplf4* seedlings exogenously with either the EPFL4 peptide or the EPFL6 peptide for 6 h. RT-qPCR analysis revealed a significantly decreased expression of *WUS* and *CLV3* in response to both peptides (Fig. 5B). Several other genes, that have altered expression in *er erl1 erl2* such as *STM* (Fig. 1G), *MONOPTEROS (MP)* (Chen et al., 2013) and *CLV1* (Fig. S3), did not change expression after the peptide treatment (Fig. 5B), suggesting specificity in the downregulation of *CLV3* and *WUS*. The decrease in *WUS* and *CLV3* mRNA levels was dependent on the presence of functional ERf receptors, as it was not observed when *er erl1 erl2* seedlings were treated with EPFL4 (Fig. 5C).

Next, we analyzed whether the ability of EPFLs to suppress expression of *WUS* and *CLV3* is dependent on CLV3 function. The *clv3-9* allele carries a point mutation in the coding region of *CLV3* that disrupts its function but not expression. The *clv3 epfl1 epfl2 epfl4 epfl6* mutant was treated with EPFL6 for 1, 3 and 6 h. The 1 h treatment produced a statistically significant decrease in *CLV3* levels, and the 3 h treatment produced a statistically significant decrease in the *WUS* levels. Interestingly, the 6 h treatment did not lead to a further reduction of *CLV3* or *WUS* expression. At the same time, a treatment of seedlings with EPFL6 in the presence of the translational inhibitor cycloheximide had a very strong impact on the steady-state

Development (2021) 148, dev189753. doi:10.1242/dev.189753

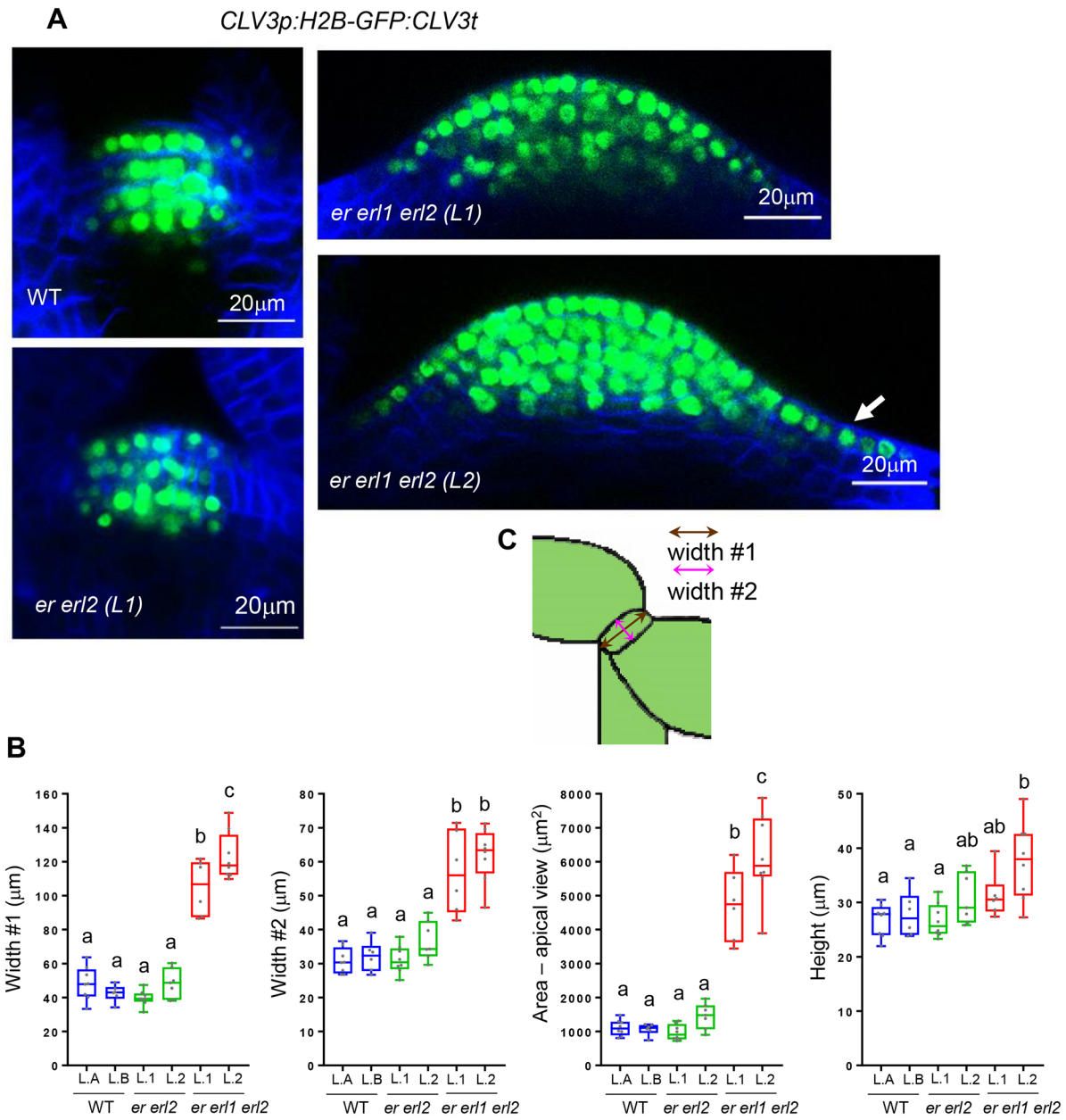

Fig. 3. Expression of CLV3 is expanded laterally in the er erl1 erl2 mutants. (A) Confocal images of the SAM region of 1 DPG wild-type (wt) and mutant seedlings transformed with *CLV3p:H2B-GFP:CLV3t* (green). The cell walls were stained with SR2200 (blue). The white arrow indicates extended expression of the reporter in the L1 layer. (B) Measurements of *CLV3p:H2B-GFP:CLV3t* expression in the SAM of WT, *er erl1 erl2* mutants and the segregating siblings of *er erl1 erl2* (*er erl2*). L.A and L.B are two independent WT lines, L.1 and L.2 are two independent mutant lines. The median is indicated as a horizontal line between two boxes, upper and lower quartiles are represented by the boxes, and the vertical lines designate the maximum and the minimum. Grey dots represent individual data points. *n*=6-8. For multiple comparisons (one-way ANOVA with Tukey post-hoc test), lower case letters are used to label means, such that bars bearing different letters are statistically different from one another with a minimum *P*-value of <0.01. (C) Schematic of the seedling meristematic zone demonstrating how width #1 and width #2 of the SAM were measured in B.

mRNA levels of *WUS* and *CLV3*. *WUS* and *CLV3* levels decreased approximately eleven and six times, respectively, after 3 h of treatment (Fig. 5D). Expression of two other analyzed genes, *MP* and *CLV1*, did not change (Fig. 5D). Collectively, our data imply that *WUS* and *CLV3* are downstream targets of the ERf signaling pathway, and the ability of ERfs to inhibit *WUS* and *CLV3* expression is independent of protein biosynthesis.

The *er erl1 erl2* mutant has a reduced sensitivity to CLV3 peptide (Kimura et al., 2018) suggesting that ERfs might have additional roles in regulation of the CLV3 signaling pathway. The reduced sensitivity of the mutant to CLV3 might be related to reduced expression of several CLV3 receptors: *CLV1*, *BAM1* and *BAM2* (Fig. S3). However, the role of ERfs in *CLV1* expression is likely to be indirect and complex. Although in the *epfl1 epfl2 epfl4* background we did not observe any effects of EPFLs on the *CLV1* expression, in *clv3 epfl1 epfl2 epfl4 epfl6* after 6 h of treatment with EPFL6 we detected, instead of an increase, a very small decrease in the *CLV1* expression (Fig. 5D).

DISCUSSION

Our analysis of genetic interactions uncovered a synergy between ERf/EPFL and CLV3 in the maintenance of SAM size and the regulation of organogenesis. Although *clv3* and *er erl1 erl2* mutants have bigger

Development (2021) 148, dev189753. doi:10.1242/dev.189753

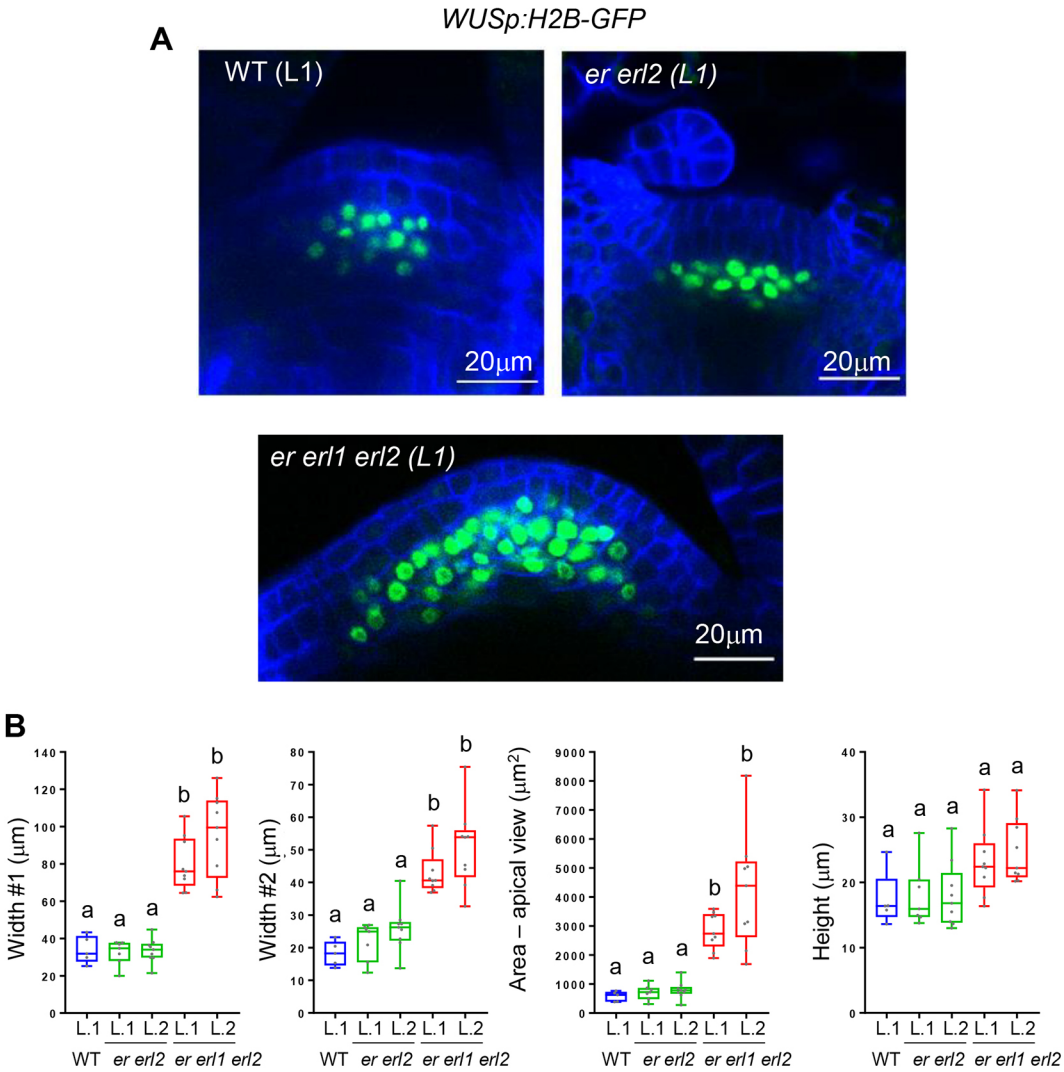

Fig. 4. Expression of *WUS* is expanded laterally in the *er erl1 erl2* mutants. (A) Confocal images of the SAM region of 1 DPG seedlings transformed with *WUSp:H2B-GFP* (green). The cell walls were stained with SR2200 (blue). (B) Measurements of *WUSp:H2B-GFP* expression in the SAM of *er erl1 erl2* mutants, their segregating siblings (*er erl2*) and F1 generation seedlings from the cross of the L.1 line with the wild type (WT). L.1 and L.2 are two independent lines. The median is indicated as a horizontal line between two boxes, upper and lower quartiles are represented by the boxes, and the vertical lines designate the maximum and the minimum. Grey dots represent individual data points. *n*=5-9. For multiple comparisons (one-way ANOVA with Tukey post-hoc test), lower case letters are used to label means, such that bars bearing different letters are statistically different from one another with a minimum *P*-value of <0.01.

SAMs, they form stems, leaves and flowers. In the quadruple mutant the growth of the meristem is unrestricted, one or two leaves form only sporadically, and cells at the periphery of the meristem are unable to differentiate into internode tissues. Synergistic phenotypes most often result from redundancy between paralogs or when pathways converge on a specific node (Pérez-Pérez et al., 2009). As WUS is the core regulator of SAM size and is the primary target of CLV3, we investigated whether the two signaling pathways converge on that transcription factor. Our genetic analysis determined that *wus* is epistatic to *er erl1 erl2* in the regulation of SAM size, suggesting that WUS could be a downstream target of the ERf/EPFL pathway. Treatment of seedlings with exogenous EPFLs for 3 or 6 h reduced steady-state levels of *WUS* mRNA only in the presence of functional ERf receptors. Considering that the average length of the cell cycle in the SAM is over 30 h (R. Jones et al., 2017), the decrease of *WUS* accumulation cannot be attributed to a decrease in the size of the SAM. Moreover, when cycloheximide was included in the treatment, EPFLs were still able to change steady-state levels of *WUS*, suggesting that EPFLs control *WUS* independently of protein biosynthesis. Consistent with previously published data (Gordon et al., 2009), we noticed an increased accumulation of *WUS* in the presence of cycloheximide (Fig. S3A). Our experiments do not distinguish whether ERf/EPFL signaling controls *WUS* transcription or its mRNA stability. We also do not know why EPFL6 has a stronger impact on *WUS* expression in the presence of cycloheximide. Perhaps there is a negative unstable regulator of *WUS*, and during cycloheximide treatment its concentration drops which enhances the impact of EPFLs on *WUS* transcription. Alternatively, an EPFL-induced increase in *WUS* mRNA degradation might be more evident if an inhibition of translation elongation alters stability of *WUS* mRNA.

It has previously been noticed that ERECTA and CLV3 function along different spatial axes: CLV3 preferentially regulates meristem height and ERECTA regulates meristem width (Mandel et al., 2016). Four ligands that regulate the activity of ERfs in the SAM are mostly expressed at the periphery of the meristem and are excluded from the central zone and organizing center (Kosentka et al., 2019).

Development (2021) 148, dev189753. doi:10.1242/dev.189753

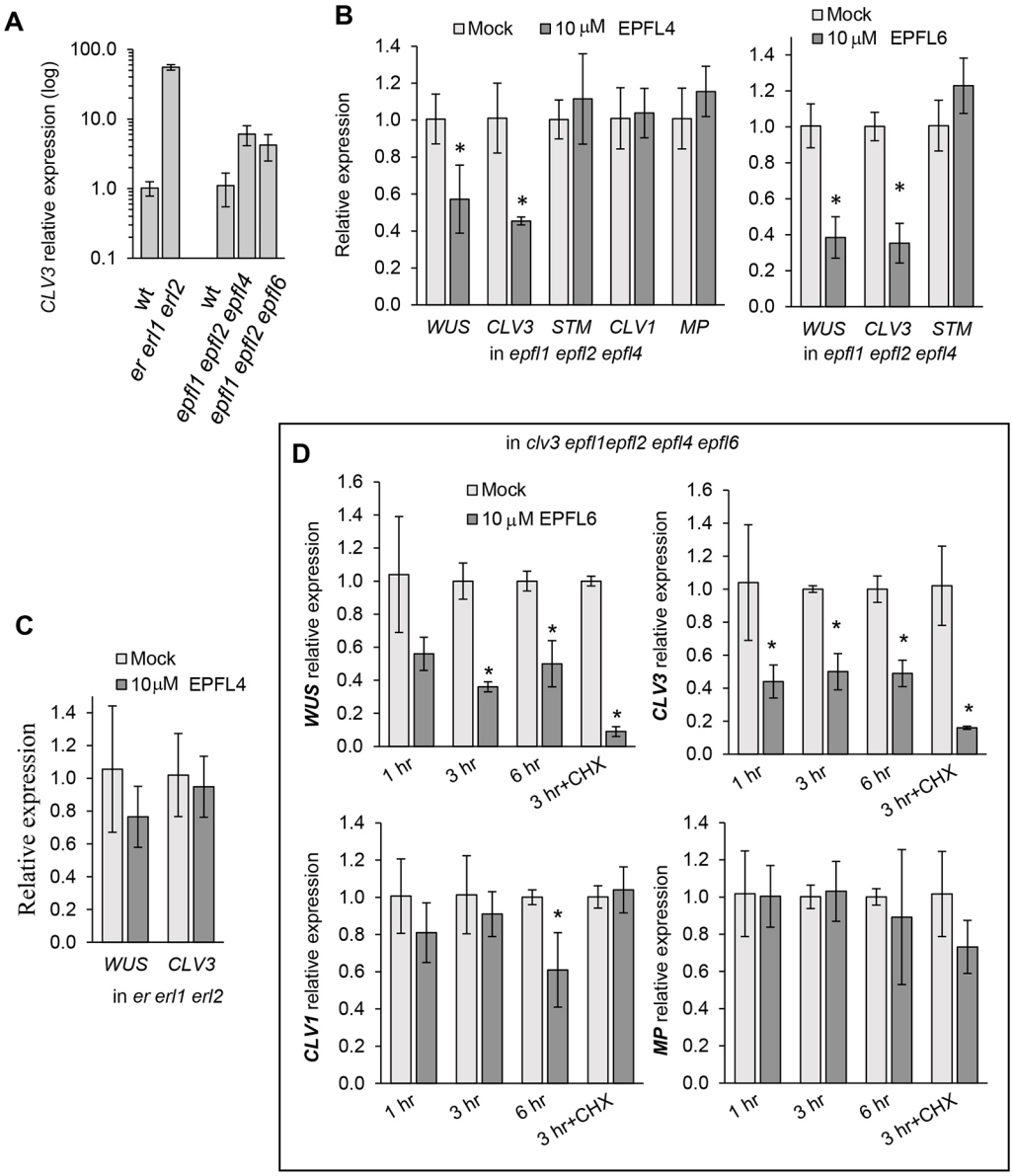

Fig. 5. *WUS* and *CLV3* are targets of the ERf signaling pathway. (A) *CLV3* relative expression levels in above-ground parts of 5 DPG seedlings in genotypes as indicated. (B-D) Relative expression levels of selected mRNAs in above-ground organs of 3 DPG *epfl1 epfl2 epfl4* (B), *er erl1 erl2* (C) or *clv3 epfl1 epfl2 epfl4 epfl6* (D) seedlings after treatment with 10 µM EPFL4 or EPFL6 peptides as indicated compared with mock treatment. Seedlings were treated with peptides for 6 h (B,C) and from 1 to 6 h as indicated (D). +CHX indicates treatment with 10 µM cycloheximide. Data are mean±s.d. *ACTIN2* was used as an internal control. **P*<0.05 (unpaired two-tailed Student's *t*-test).

EPFL1 expression in the peripheral zone under the *KANADI* promoter fully rescues meristematic defects of *epfl1 epfl2 epfl4 epfl6* (Kosentka et al., 2019). In contrast, although ERfs are endogenously expressed throughout the SAM, their function in the center of the meristem is crucial for SAM maintenance. *ERECTA* expressed under the *CLV3* promoter rescues meristematic defects significantly better compared with its expression under the *KANADI* promoter (Kosentka et al., 2019). The distinct expression of ERfs and EPFLs in the SAM is similar to their distinct expression during leaf tooth initiation, in which ERfs are expressed more strongly at the tip of the tooth, whereas EPFL2 is excluded from the tip and is expressed in the surrounding sinus tissues (Tameshige et al., 2016). Expression of *ERECTA* under the *DR5* promoter exclusively at the tip of the leaf tooth rescues its growth (Tameshige et al., 2016), just as expression of *ERECTA* under the *CLV3* promoter in the center of the meristem rescues meristematic phenotypes (Kosentka et al., 2019). Previously, we have proposed that the signaling occurs in the peripheral region of the SAM where expression of EPFL and ERf overlaps, a pattern similar to that observed in the leaf tooth. The present quantitative analysis of *CLV3* and *WUS* expression in the *er erl1 erl2* mutant confirms that ERf functions in restricting their expression laterally.

We propose that ERfs restrict the size of the central zone by inhibiting expression of *CLV3* and *WUS* in the periphery of the SAM (Fig. 6). This control is especially important during establishment of the SAM during embryogenesis. After germination, CLV3 signaling can partially substitute for ERfs in the lateral inhibition of *WUS* expression. However, when both signaling pathways are disrupted, as in the *clv3 er erl1 erl2* mutant, *WUS* expression becomes rampant, and the SAM expands without restraint. Increased expression of *CLV3* in the L1 layer of *er erl1erl2* and *wus er erl1 erl2* (Kimura et al., 2018) suggests that an as-yet unidentified signal induces *CLV3* expression in the epidermis, consistent with a previously proposed model (Gruel et al., 2016).

Our recent mathematical model describing regulatory networks in the SAM identified nonlinear cooperativity of EPFL and CLV3 signals in the control of the lateral boundary of *WUS* expression (Liu et al., 2020). The model demonstrates the paradoxical role of EPFLs in regulation of *WUS* expression: they directly downregulate *WUS* and, at the same time, they upregulate it by inhibiting expression of

Development (2021) 148, dev189753. doi:10.1242/dev.189753

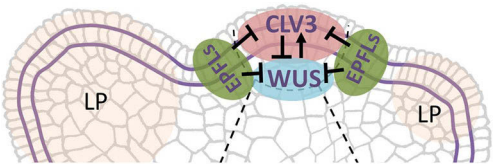

Fig. 6. Model for the role of ERf signaling in regulation of shoot meristem maintenance. EPFL signals originating from the periphery of the SAM activate the ERf signaling cascade that restricts the expression of *CLV3* and *WUS* to the center of the SAM. LP, leaf primordium.

CLV3. The downregulation plays the dominant role, as blocking it in the model leads to expression patterns very similar to the *er erl1 erl2* mutant. The model also suggested that the inhibition of *CLV3* expression by EPFLs is necessary to shift *CLV3* expression vertically from the organizing center to the top of the SAM.

MATERIALS AND METHODS

Plant materials and growth conditions

The *Arabidopsis thaliana* ecotype Columbia was used as the wild type. The following mutants used in the study have been described previously: *er-105 erl1-2 erl2-1* (Shpak et al., 2004), *epfl1 epfl2 epfl4*, *epfl1 epfl2 epfl6* and *epfl1 epfl2 epfl4 epfl6* (Kosentka et al., 2019), *clv3-9* (Nimchuk et al., 2015) and *wus* null allele (SAIL_150_G06; Sonoda et al., 2007). They are all in the Columbia background.

To create *clv3 er erl2*, *clv3 er erl1 erl2* and *wus er erl1 erl2* plants, *clv3-9* and *wus/+* were crossed with *er erl1/+ erl2*. To create *wus clv3* plants, *clv3-9* was crossed with *wus/+*. To create *wus clv3 er erl1 erl2* plants *clv3 er erl1/+ erl2* was crossed with *wus/+ er erl1/+ erl2*. The higher-order mutants were identified in subsequent generations based on the phenotype. The homozygous status of *wus* and *erl1* were confirmed when necessary by genotyping as described previously (Kosentka et al., 2017; Sonoda et al., 2007). To create *clv3 epfl1 epfl2 epfl4 epfl6* plants, the *clv3-9* mutant was crossed with *epfl1/+ epfl2 epfl4 epfl6.* The *epfl* mutations were genotyped as described previously (Kosentka et al., 2019).

The *WUSp:H2B-GFP:35St* construct (pESH 746) was created by fusing the 4.5 kb sequence of the *WUS* promoter (Yadav et al., 2009) with *H2B-EGFP* and the *35S* terminator. The *CLV3p:H2B-GFP:CLV3t* construct (pESH 747) was created by fusing the 1.5 kb sequence of the *CLV3* promoter with *H2B-EGFP* and the 1.2 kb *CLV3* terminator. The inserts were generated by overlap extension PCR and inserted into the binary vector pPZP222 between BamHI and SalI restiction sites. The template for amplifying the H2B-EGFP sequence was a plasmid from the Z. Nimchuk lab (UNC Chapel Hill, USA). Both constructs were examined by sequencing of amplified regions. The pESH746 and pESH747 were transformed into an *Agrobacterium tumefaciens* strain GV3101/pMP90 by electroporation and introduced into the wild type (Columbia ecotype) and er erl1/+ erl2 plants by the floral dip method. T1 transgenic plants were selected using gentamycin resistance. Heterozygous erl1/+ plants in the T1 generation were identified by genotyping.

Plants were grown as previously described (Kosentka et al., 2017) under an 18 h light/6 h dark cycle (long days) at 21°C. For analysis of SAM size and leaf initiation seedlings were grown on modified Murashige and Skoog medium plates supplemented with 1% (w/v) sucrose. For all experiments, seeds were stratified for 2 days at 4°C before germination.

To analyze expression of genes after EPFL4 and EPFL6 treatment, *epfl1 epfl2 epfl4* mutants were grown on modified Murashige and Skoog medium plates for 5 days (3 DPG). Then 60 seedlings (EPFL4 treatment) or 10 seedlings (EPFL6 treatment) per biological replicate were transferred to 1 ml of liquid Murashige and Skoog medium containing 10 µM of EPFL4 or EPFL6. The purification of EPFL4 and EPFL6 peptides has been described previously (Lin et al., 2017). EPFL peptides were dissolved in 10 mM Bis-Tris, 100 mM NaCl (pH 6.0). For mock treatment, a buffer solution of equal volume was added to the medium (92.6 µl in the EPFL4 experiment and 8.7 µl in the EPFL6 experiment). To analyze the effect of EPFL6 in the presence of cycloheximide, seedlings were incubated for 10 min in Murashige and Skoog medium containing 10 µM cycloheximide and then 10 µM of EPFL6 was added to the 'treatment' group. For each treatment there were three biological replicas.

Microscopy

To measure leaf initiation and SAM size, one, three and five DPG seedlings were fixed overnight with ethanol: acetic acid [9:1 (v/v)]. After fixation, samples were rehydrated with an ethanol series to 30% (v/v) ethanol and cleared in chloral hydrate solution. Chloral hydrate:water:glycerol 8:1:1 (w/v/v) solution contained KOH at 10 mM concentration to prevent degradation of tissues due to high acidity of chloral hydrate. In our experience the acidity of chloral hydrate (Sigma-Aldrich) varies from batch to batch, and the necessity to add KOH should be tested experimentally. Microscopic observations of meristematic regions by DIC microscopy were performed as described previously (Chen et al., 2013). Tissue samples were fixed overnight in acetic acid:ethanol (1:9) at room temperature, dehydrated with a graded series of ethanol, and infiltrated with polymethacryl resin Technovit 7100 (Heraeus Kulzer) followed by embedding and polymerization in Technovit 7100. Then, 7 µm sections were prepared using a Leica RM-6145 microtome. The tissue sections were stained with 0.02% Toluidine Blue O and observed under bright-field illumination. Pictures of older seedlings and the analysis of flower structure was carried out using a Leica MZ16 FA stereomicroscope.

Imaging of the SAMs in T2 plants expressing *WUSp:H2B-GFP:35St* or *CLV3p:H2B-GFP:CLV3t* was carried out using a Leica SP8 White Light Laser Confocal microscope. EGFP was excited using a 488-nm White Light Supercontinuum Laser (Leica Microsystems). SCRI Renaissance 2200 (SR2200) was excited with a Diode 405 nm 'UV' laser (Leica Microsystems). EGFP and SR2200 fluorescence emission was collected with HyD 'Hybrid' Super Sensitivity SP Detector (Leica Microsystems) and PMT SP Detector (Leica Microsystems). Sequential line scanning was used to generate *z*-stacks. For better observation of fluorescence in the SAM of live 1-day old seedlings, one cotyledon was removed before imaging. SR2200 (Renaissance Chemicals) was prepared as in Musielak et al. (2015) except for the omission of paraformaldehyde. Samples were incubated in ~350-500 µl of staining solution under vacuum for ~1-2 min at room temperature, washed with 1× PBS buffer to remove excess dye, and imaged.

The Fiji image processing package was used for all quantitative image measurements. Two-dimensional slices were used to measure the height of reporter expression in *WUSp:H2B-GFP:35St* plants. Three dimensional images were used for all other measurements. Apical area measurements were acquired by drawing a circle around the expression domain using the freehand measurement tool and data were analyzed using one-way ANOVA with Tukey's post-hoc test. The *er erl1 erl2* mutants in the T2 generation were identified based on stomata clustering.

Quantitative RT-PCR analysis

Total RNA was isolated from the above-ground tissues of seedlings using the Spectrum Plant RNA Isolation Kit (Sigma-Aldrich). The RNA was treated with RNase-free RQ1 DNase (Promega). First-strand complementary cDNA was synthesized with LunaScript™ RT SuperMix Kits (New England Biolabs). Quantitative PCR was performed with a CFX96 Touch Real-Time PCR Detection System (Bio-Rad) using Sso Fast EvaGreen Supermix (Bio-Rad). Each experiment contained three technical replicates of three biological replicates and was performed in a total volume of 10 µl with 4 µl of 10× or 50× diluted cDNA. Cycling conditions were as follows: 3 min at 95°C; then 40 repeats of 10 s at 95°C, 10 s at 52°C for *ACTIN2* and *STM*; 10 s at 55°C for *WUS*; 10 s at 57°C for *MP*; 10 s at 50°C for *CLV1*, *BAM1*, *BAM2* and *BAM3*, and 10 s at 68°C, followed by the melt-curve analysis. Cycling conditions for *CLV3* were 3 min at 95°C; then 40 cycles of 95°C for 10 s and 60°C for 10 s, followed by the melt-curve analysis. Primers for *ACTIN2*, *STM*, *WUS* and *MP* (Chen et al., 2013) as well as for *CLV3* (Chiu et al., 2007) have been described previously. Primers for *CLV1*, *BAM1*, *BAM2* and *BAM3* were as in Nimchuk et al. (2015). The fold difference in gene expression was calculated using relative quantification by the $2^{-\Delta\Delta CT}$ algorithm.

Acknowledgements

We thank Zachary Nimchuk for sharing with us seeds of *clv3-9* and *wus* (SAIL_150_G06) and a construct containing the H2B-EGFP sequence. We thank Richard Maradiaga and Timothy Herman for technical assistance.

Competing interests
The authors declare no competing or financial interests.

Author contributions
Conceptualization: L.Z., E.D.S.; Methodology: L.Z.; Validation: L.Z., D.D.; Formal analysis: L.Z., D.D., E.D.S.; Investigation: L.Z., D.D., G.L., E.D.S.; Resources: G.L., J.C.; Writing - original draft: L.Z., E.D.S.; Writing - review & editing: L.Z., D.D., J.C., E.D.S.; Visualization: L.Z., D.D., E.D.S.; Supervision: J.C., E.D.S.; Project administration: J.C., E.D.S.; Funding acquisition: J.C., E.D.S.

Funding
This work was funded by the Hunsicker Research Incentive Award (University of Tennessee, Knoxville, USA) and the National Science Foundation (IOS-2016756 to E.D.S.).

Supplementary information
Supplementary information available online at
https://dev.biologists.org/lookup/doi/10.1242/dev.189753.supplemental

Peer review history
The peer review history is available online at
https://dev.biologists.org/lookup/doi/10.1242/dev.189753.reviewer-comments.pdf

References
Bergmann, D. C., Lukowitz, W. and Somerville, C. R. (2004). Stomatal development and pattern controlled by a MAPKK Kinase. *Science* **304**, 1494-1497. doi:10.1126/science.1096014

Brand, U., Fletcher, J. C., Hobe, M., Meyerowitz, E. M. and Simon, R. (2000). Dependence of stem cell fate in Arabidopsis on a feedback loop regulated by CLV3 activity. *Science* **289**, 617-619. doi:10.1126/science.289.5479.617

Chen, M.-K., Wilson, R. L., Palme, K., Ditengou, F. A. and Shpak, E. D. (2013). ERECTA family genes regulate auxin transport in the shoot apical meristem and forming leaf primordia. *Plant Physiol.* **162**, 1978-1991. doi:10.1104/pp.113.218198

Chickarmane, V. S., Gordon, S. P., Tarr, P. T., Heisler, M. G. and Meyerowitz, E. M. (2012). Cytokinin signaling as a positional cue for patterning the apical-basal axis of the growing Arabidopsis shoot meristem. *Proc. Natl. Acad. Sci. USA* **109**, 4002. doi:10.1073/pnas.1200636109

Chiu, W.-H., Chandler, J., Cnops, G., Van Lijsebettens, M. and Werr, W. (2007). Mutations in the TORNADO2 gene affect cellular decisions in the peripheral zone of the shoot apical meristem of Arabidopsis thaliana. *Plant Mol. Biol.* **63**, 731-744. doi:10.1007/s11103-006-9105-z

Daum, G., Medzihradszky, A., Suzaki, T. and Lohmann, J. U. (2014). A mechanistic framework for noncell autonomous stem cell induction in Arabidopsis. *Proc. Natl. Acad. Sci. USA* **111**, 14619-14624. doi:10.1073/pnas.1406446111

DeYoung, B. J., Bickle, K. L., Schrage, K. J., Muskett, P., Patel, K. and Clark, S. E. (2006). The CLAVATA1-related BAM1, BAM2 and BAM3 receptor kinase-like proteins are required for meristem function in Arabidopsis. *Plant J.* **45**, 1-16. doi:10.1111/j.1365-313X.2005.02592.x

Fletcher, J. C., Brand, U., Running, M. P., Simon, R. and Meyerowitz, E. M. (1999). Signaling of cell fate decisions by CLAVATA3 in Arabidopsis shoot meristems. *Science* **283**, 1911-1914. doi:10.1126/science.283.5409.1911

Fuchs, M. and Lohmann, J. U. (2020). Aiming for the top: non-cell autonomous control of shoot stem cells in Arabidopsis. *J. Plant Res.* **133**, 297-309. doi:10.1007/s10265-020-01174-3

Gordon, S. P., Chickarmane, V. S., Ohno, C. and Meyerowitz, E. M. (2009). Multiple feedback loops through cytokinin signaling control stem cell number within the Arabidopsis shoot meristem. *Proc. Natl. Acad. Sci. USA* **106**, 16529-16534. doi:10.1073/pnas.0908122106

Gruel, J., Landrein, B., Tarr, P., Schuster, C., Refahi, Y., Sampathkumar, A., Hamant, O., Meyerowitz, E. M. and Jönsson, H. (2016). An epidermis-driven mechanism positions and scales stem cell niches in plants. *Sci. Adv.* **2**, e1500989. doi:10.1126/sciadv.1500989

Gruel, J., Deichmann, J., Landrein, B., Hitchcock, T. and Jönsson, H. (2018). The interaction of transcription factors controls the spatial layout of plant aerial stem cell niches. *NPJ Syst. Biol. Appl.* **4**, 36. doi:10.1038/s41540-018-0072-1

Hara, K., Kajita, R., Torii, K. U., Bergmann, D. C. and Kakimoto, T. (2007). The secretory peptide gene EPF1 enforces the stomatal one-cell-spacing rule. *Genes Dev.* **21**, 1720-1725. doi:10.1101/gad.1550707

Hara, K., Yokoo, T., Kajita, R., Onishi, T., Yahata, S., Peterson, K. M., Torii, K. U. and Kakimoto, T. (2009). Epidermal cell density is autoregulated via a secretory peptide, EPIDERMAL PATTERNING FACTOR 2 in Arabidopsis leaves. *Plant Cell Physiol.* **50**, 1019-1031. doi:10.1093/pcp/pcp068

Hu, C., Zhu, Y., Cui, Y., Cheng, K., Liang, W., Wei, Z., Zhu, M., Yin, H., Zeng, L., Xiao, Y. et al. (2018). A group of receptor kinases are essential for CLAVATA signalling to maintain stem cell homeostasis. *Nat. Plants* **4**, 205-211. doi:10.1038/s41477-018-0123-z

Kimura, Y., Tasaka, M., Torii, K. U. and Uchida, N. (2018). ERECTA-family genes coordinate stem cell functions between the epidermal and internal layers of the shoot apical meristem. *Development* **145**, dev156380. doi:10.1242/dev.156380

Kinoshita, A., Betsuyaku, S., Osakabe, Y., Mizuno, S., Nagawa, S., Stahl, Y., Simon, R., Yamaguchi-Shinozaki, K., Fukuda, H. and Sawa, S. (2010). RPK2 is an essential receptor-like kinase that transmits the CLV3 signal in Arabidopsis. *Development* **137**, 3911-3920. doi:10.1242/dev.048199

Klawe, F. Z., Stiehl, T., Bastian, P., Gaillochet, C., Lohmann, J. U. and Marciniak-Czochra, A. (2020). Mathematical modeling of plant cell fate transitions controlled by hormonal signals. *PLoS Comput. Biol.* **16**, e1007523. doi:10.1371/journal.pcbi.1007523

Kosentka, P. Z., Zhang, L., Simon, Y. A., Satpathy, B., Maradiaga, R., Mitoubsi, O. and Shpak, E. D. (2017). Identification of critical functional residues of receptor-like kinase ERECTA. *J. Exp. Bot.* **68**, 1507-1518. doi:10.1093/jxb/erx022

Kosentka, P. Z., Overholt, A., Maradiaga, R., Mitoubsi, O. and Shpak, E. D. (2019). EPFL signals in the boundary region of the SAM restrict its size and promote leaf initiation. *Plant Physiol.* **179**, 265. doi:10.1104/pp.18.00714

Lampard, G. R., Lukowitz, W., Ellis, B. E. and Bergmann, D. C. (2009). Novel and expanded roles for MAPK signaling in Arabidopsis stomatal cell fate revealed by cell type–specific manipulations. *Plant Cell* **21**, 3506. doi:10.1105/tpc.109.070110

Lampard, G. R., Wengier, D. L. and Bergmann, D. C. (2014). Manipulation of mitogen-activated protein kinase kinase signaling in the Arabidopsis stomatal lineage reveals motifs that contribute to protein localization and signaling specificity. *Plant Cell* **26**, 3358. doi:10.1105/tpc.114.127415

Laux, T., Mayer, K. F., Berger, J. and Jurgens, G. (1996). The WUSCHEL gene is required for shoot and floral meristem integrity in Arabidopsis. *Development* **122**, 87-96.

Lee, J. S., Kuroha, T., Hnilova, M., Khatayevich, D., Kanaoka, M. M., McAbee, J. M., Sarikaya, M., Tamerler, C. and Torii, K. U. (2012). Direct interaction of ligand-receptor pairs specifying stomatal patterning. *Genes Dev.* **26**, 126-136. doi:10.1101/gad.179895.111

Lin, G., Zhang, L., Han, Z., Yang, X., Liu, W., Li, E., Chang, J., Qi, Y., Shpak, E. D. and Chai, J. (2017). A receptor-like protein acts as a specificity switch for the regulation of stomatal development. *Genes Dev.* **31**, 927-938. doi:10.1101/gad.297580.117

Liu, Z., Shpak, E. D. and Hong, T. (2020). A mathematical model for understanding synergistic regulations and paradoxical feedbacks in the shoot apical meristem. *Comput. Struct. Biotechnol. J.* **18**, 3877-3889. doi:10.1016/j.csbj.2020.11.017

Mandel, T., Candela, H., Landau, U., Asis, L., Zelinger, E., Carles, C. C. and Williams, L. E. (2016). Differential regulation of meristem size, morphology and organization by the ERECTA, CLAVATA and class III HD-ZIP pathways. *Development* **143**, 1612. doi:10.1242/dev.129973

Mayer, K. F. X., Schoof, H., Haecker, A., Lenhard, M., Jürgens, G. and Laux, T. (1998). Role of WUSCHEL in regulating stem cell fate in the Arabidopsis shoot meristem. *Cell* **95**, 805-815. doi:10.1016/S0092-8674(00)81703-1

Meng, X., Wang, H., He, Y., Liu, Y., Walker, J. C., Torii, K. U. and Zhang, S. (2012). A MAPK cascade downstream of ERECTA receptor-like protein kinase regulates Arabidopsis inflorescence architecture by promoting localized cell proliferation. *Plant Cell* **24**, 4948-4960. doi:10.1105/tpc.112.104695

Min, Y. and Kramer, E. M. (2020). Transcriptome profiling and weighted gene co-expression network analysis of early floral development in Aquilegia coerulea. *Sci. Rep.* **10**, 19637. doi:10.1038/s41598-020-76750-7

Müller, R., Borghi, L., Kwiatkowska, D., Laufs, P. and Simon, R. (2006). Dynamic and compensatory responses of Arabidopsis shoot and floral meristems to CLV3 signaling. *Plant Cell* **18**, 1188. doi:10.1105/tpc.105.040444

Müller, R., Bleckmann, A. and Simon, R. (2008). The receptor Kinase CORYNE of Arabidopsis transmits the stem cell–limiting signal CLAVATA3 independently of CLAVATA1. *Plant Cell* **20**, 934. doi:10.1105/tpc.107.057547

Musielak, T. J., Schenkel, L., Kolb, M., Henschen, A. and Bayer, M. (2015). A simple and versatile cell wall staining protocol to study plant reproduction. *Plant Reprod.* **28**, 161-169. doi:10.1007/s00497-015-0267-1

Nimchuk, Z. L., Zhou, Y., Tarr, P. T., Peterson, B. A. and Meyerowitz, E. M. (2015). Plant stem cell maintenance by transcriptional cross-regulation of related receptor kinases. *Development* **142**, 1043-1049. doi:10.1242/dev.119677

Pérez-Pérez, J. M., Candela, H. and Micol, J. L. (2009). Understanding synergy in genetic interactions. *Trends Genet.* **25**, 368-376. doi:10.1016/j.tig.2009.06.004

R. Jones, A., Forero-Vargas, M., Withers, S. P., Smith, R. S., Traas, J., Dewitte, W. and Murray, J. A. H. (2017). Cell-size dependent progression of the cell cycle creates homeostasis and flexibility of plant cell size. *Nat. Commun.* **8**, 15060. doi:10.1038/ncomms15060

Schoof, H., Lenhard, M., Haecker, A., Mayer, K. F. X., Jürgens, G. and Laux, T. (2000). The stem cell population of Arabidopsis shoot meristems is maintained by a regulatory loop between the CLAVATA and WUSCHEL Genes. *Cell* **100**, 635-644. doi:10.1016/S0092-8674(00)80700-X

Shinohara, H. and Matsubayashi, Y. (2015). Reevaluation of the CLV3-receptor interaction in the shoot apical meristem: dissection of the CLV3 signaling pathway from a direct ligand-binding point of view. *Plant J.* **82**, 328-336. doi:10.1111/tpj.12817

Development (2021) 148, dev189753. doi:10.1242/dev.189753

Shpak, E. D. (2013). Diverse roles of ERECTA family genes in plant development. *J. Integr. Plant Biol.* **55**, 1238-1250. doi:10.1111/jipb.12108

Shpak, E. D., Berthiaume, C. T., Hill, E. J. and Torii, K. U. (2004). Synergistic interaction of three ERECTA-family receptor-like kinases controls Arabidopsis organ growth and flower development by promoting cell proliferation. *Development* **131**, 1491-1501. doi:10.1242/dev.01028

Sonoda, Y., Yao, S.-G., Sako, K., Sato, T., Kato, W., Ohto, M.-a., Ichikawa, T., Matsui, M., Yamaguchi, J. and Ikeda, A. (2007). SHA1, a novel RING finger protein, functions in shoot apical meristem maintenance in Arabidopsis. *Plant J.* **50**, 586-596. doi:10.1111/j.1365-313X.2007.03062.x

Tameshige, T., Okamoto, S., Lee, J. S., Aida, M., Tasaka, M., Torii, Keiko, U. and Uchida, N. (2016). A secreted peptide and its receptors shape the auxin response pattern and leaf margin morphogenesis. *Curr. Biol.* **26**, 2478-2485. doi:10.1016/j.cub.2016.07.014

Uchida, N., Shimada, M. and Tasaka, M. (2013). ERECTA-family receptor kinases regulate stem cell homeostasis via buffering its Cytokinin responsiveness in the shoot apical meristem. *Plant Cell Physiol.* **54**, 343-351. doi:10.1093/pcp/pcs109

Vernoux, T., Kronenberger, J., Grandjean, O., Laufs, P. and Traas, J. (2000). PIN-FORMED 1 regulates cell fate at the periphery of the shoot apical meristem. *Development* **127**, 5157-5165.

Wang, H., Ngwenyama, N., Liu, Y., Walker, J. C. and Zhang, S. (2007). Stomatal development and patterning are regulated by environmentally responsive mitogen-activated protein kinases in Arabidopsis. *Plant Cell* **19**, 63-73. doi:10.1105/tpc.106.048298

Yadav, R. K., Girke, T., Pasala, S., Xie, M. and Reddy, G. V. (2009). Gene expression map of the Arabidopsis shoot apical meristem stem cell niche. *Proc. Natl. Acad. Sci. USA* **106**, 4941-4946. doi:10.1073/pnas.0900843106

Yadav, R. K., Perales, M., Gruel, J., Girke, T., Jönsson, H. and Reddy, G. V. (2011). WUSCHEL protein movement mediates stem cell homeostasis in the Arabidopsis shoot apex. *Genes Dev.* **25**, 2025-2030. doi:10.1101/gad.17258511

Zhou, Y., Yan, A., Han, H., Li, T., Geng, Y., Liu, X. and Meyerowitz, E. M. (2018). HAIRY MERISTEM with WUSCHEL confines CLAVATA3 expression to the outer apical meristem layers. *Science* **361**, 502. doi:10.1126/science.aar8638